Electronic Supplementary Information

Copper-free and enzyme-free click chemistry-mediated single quantum dot nanosensor for accurate detection of microRNAs in cancer cells and tissues

Zi-yue Wang,‡[a] Dong-ling Li,‡[a] Xiaorui Tian,‡[a] Chun-yang Zhang*[a]

[a] College of Chemistry, Chemical Engineering and Materials Science, Collaborative Innovation Center of Functionalized Probes for Chemical Imaging in Universities of Shandong, Key Laboratory of Molecular and Nano Probes, Ministry of Education, Shandong Provincial Key Laboratory of Clean Production of Fine Chemicals, Shandong Normal University, Jinan 250014, China.

* Correspondence should be addressed to cyzhang@sdnu.edu.cn.

‡ These authors contributed equally.

Normalized absorption and emission spectra of the 605QD and Cy5.

In this assay, we selected the 605 nm-emitting QD as the energy donor and Cy5 as the energy acceptor based on following reasons: (1) the emission of QD (Figure S1, red line) and the emission of Cy5 (Figure S1, pink line) exhibit negligible cross-talk, and there is significant absorption spectral overlap between the emission spectrum of QDs (Figure S1, red line) and the absorption spectrum of Cy5 (Figure S1, blue line), enabling efficient FRET from the QD donor to Cy5 acceptor at the excitation wavelength of 488 nm; (2) the QD has the capability of assembling multiple Cy5/biotin-modified oligonucleotides onto the surface of single QD to obtain a single-donor/multiple-acceptor nanostructure for improved FRET efficiency; (3) the measured Cy5 signals are exclusively caused by FRET effect, because Cy5 cannot be excited by the 488 nm laser. (4) Based on the distance between the adjacent DNA bases is 0.34 nm in dsDNA and the radius of streptavidin-coated QD conjugate is 5.0-7.5 nm, the total length of the resultant QD-oligonucleotides-Cy5 nanostructure is calculated to be 12.94 nm, within the efficient FRET range ($2R_0$ = 15.4 nm).

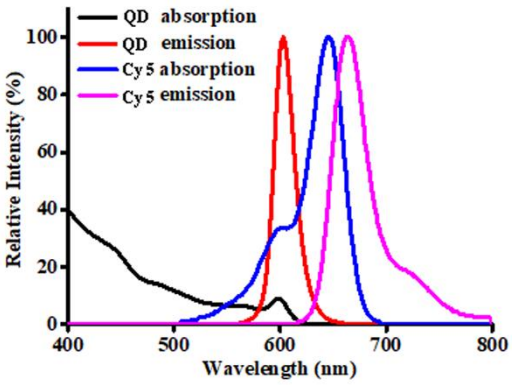

Figure S1. Normalized absorption and emission spectra of the 605 nm-emitting QD and Cy5. Black line, absorption spectrum of the 605 nm-emitting QD; red line, emission spectrum of the 605 nm-emitting QD; blue line, absorption spectrum of Cy5; magenta line, emission spectrum of Cy5.

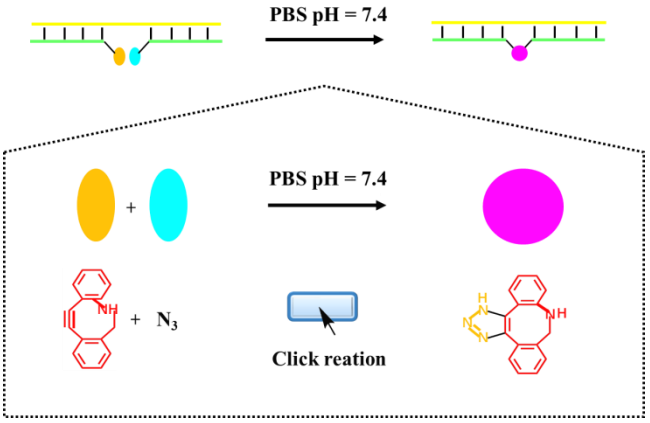

Scheme S1. Structure diagram of the click chemical reaction.

Optimization of the thermal cycle number.

In the proposed assay, the thermal cycle number of enzyme-free cycling click chemistry-mediated tricyclic LCR amplification plays a crucial role in miRNA-155 detection. Therefore, the thermal cycle number should be optimized. As shown in Fig. S2, the Cy5 fluorescence intensity enhances quickly with the increasing number of thermal cycles from 20 to 50 and reaches its peak when the cycle number is 50. Therefore, 50 cycles are selected as the optimal thermal cycle number in the tricyclic LCR amplification.

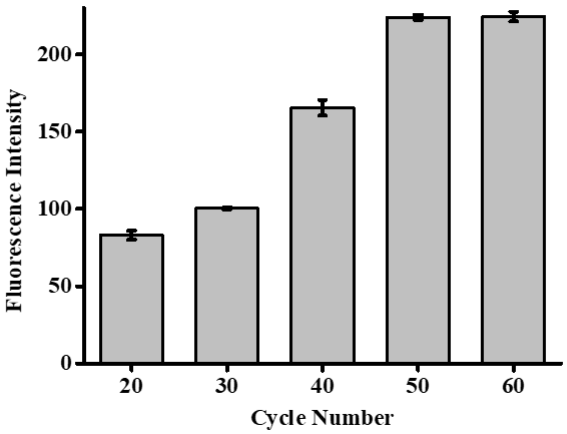

Figure S2. Variance of Cy5 fluorescence intensity with reaction cycle number of enzyme-free cycling click chemistry-mediated tricyclic LCR amplification. The miRNA-155 concentration is 10 nM. The concentration of each DNA probes is 100 nM. Error bars show the standard deviation of three experiments.

Optimization of the concentration of DNA probes.

The concentration of DNA probes (i.e., DNA probes 1, 2, 3 and 4) in the LCR amplification is very important for the amplification efficiency. Therefore, the concentration of each DNA probes (i.e., DNA probes 1, 2, 3 and 4) should be optimized. As shown in Fig. S3, the Cy5 fluorescence intensity enhances quickly with the increasing concentration of each DNA probes (i.e., DNA probes 1, 2, 3 and 4) from 30 to 100 nM under the condition that the ratio of four DNA probes is 1:1:1:1, and the Cy5 fluorescence intensity reaches its peak when the concentration of each DNA probes (i.e., DNA probes 1, 2, 3 and 4) is 100 nM. Therefore, 100 nM is selected as the optimal concentration of each DNA probes of DNA probes (i.e., DNA probes 1, 2, 3 and 4) in the tricyclic LCR amplification.

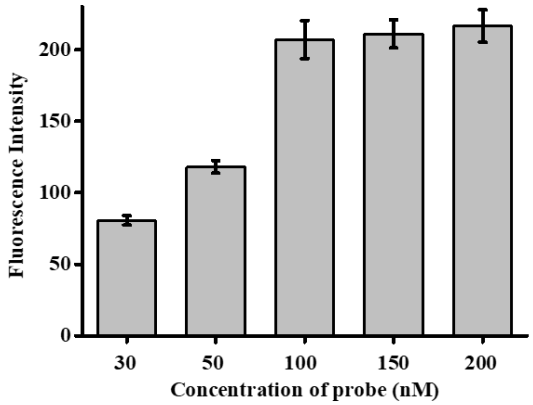

Figure S3. Variance of Cy5 fluorescence intensity with concentration of each DNA probes (i.e., DNA probes 1, 2, 3 and 4) under the condition that the ratio of four DNA probes is 1:1:1:1. The miRNA-155 concentration is 10 nM. Error bars show the standard deviation of three experiments.

Optimization of the pH of PBS.

The incubation environment of enzyme-free cycling click chemistry-mediated tricyclic LCR is essential to the amplification efficiency. Therefore, the pH of PBS should be optimized. As shown in Fig. S4, the Cy5 fluorescence intensity increases with pH of PBS from 6 to 7.4 and reaches its peak when pH of PBS is 7.4. Therefore, 7.4 is selected as the optimal pH of PBS in the tricyclic LCR amplification.

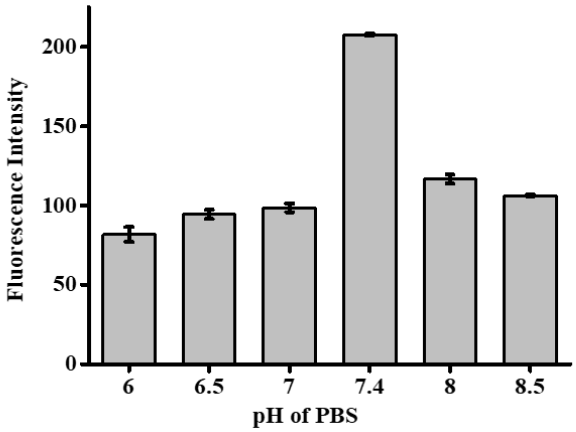

Figure S4. Variance of Cy5 fluorescence intensity with pH of PBS. The miRNA-155 concentration is 10nM. The concentration of each DNA probes is 100 nM. Error bars show the standard deviation of three experiments.

Influence of QD-to-Cy5-labled substrate ratio on FRET efficiency.

We employed the fluorescence measurement to optimize the QD-to-Cy5-labled substrate ratio. As shown in Figure S5, both the FRET efficiency and the Cy5 fluorescence intensity enhances with the increasing ratio of the QD-to-Cy5-labled substrate ratio from 6 to 36, and reach a plateau beyond the ratio of 36, indicating that the biotin-binding sites on the surface of the QD have been saturated, which is close to the theoretically calculated biotin-binding sites per QD of 36−45.[1] Because of the assembly of 3 available biotin binding sites per streptavidin and 12−15 streptavidins per QD, there are 36-45 biotin-binding sites per QD in theory.[2] Thus, the QD-to-Cy5-labled substrate ratio of 36 is used in the subsequent research.

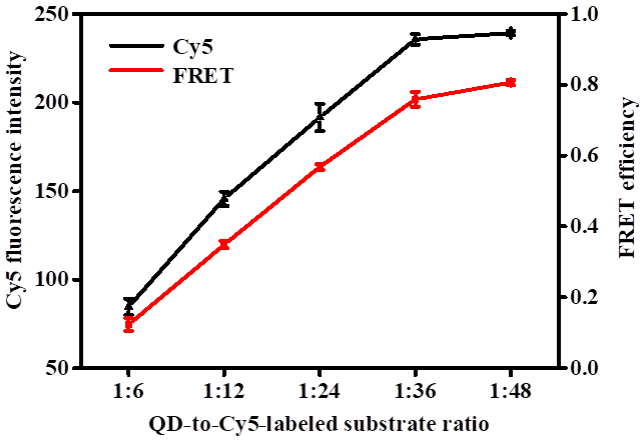

Figure S5. Variance of FRET efficiency (red color) and Cy5 fluorescence intensity (black color) as a function of the QD-to-Cy5-labeled substrate ratio. The concentration of QD is 2.78 nM. Error bars show the standard deviation of three experiments.

The fluorescence intensity induced by different-concentration miRNA-155.

We evaluate the fluorescence intensity induced by different-concentration miRNA-155 under the optimized experimental conditions (Figures S2-S5). As shown in Figure S6A, the QD fluorescence intensity decreases with the increasing concentration of miRNA-155 in a range of 1×10^{-16} – 1×10^{-8} M, accompanied by an increase of Cy5 fluorescence intensity correspondingly. A good linear correlation is obtained between the F-F_0 of QD and the logarithm of miRNA-155 concentration in the range from 1×10^{-16} – 1×10^{-8} M (Figure S6B). The regression equation is $F_0 - F = 10212.95 + 642.51 \log_{10}C$ ($R^2 = 0.9946$), where C is the miRNA-155 concentration, F and F_0 are the fluorescence intensity of QD in the presence and absence of target miRNA-155, respectively. The limit of detection (LOD) is measured to be 1.27×10^{-16} M by calculating the control group plus three times the standard deviation.

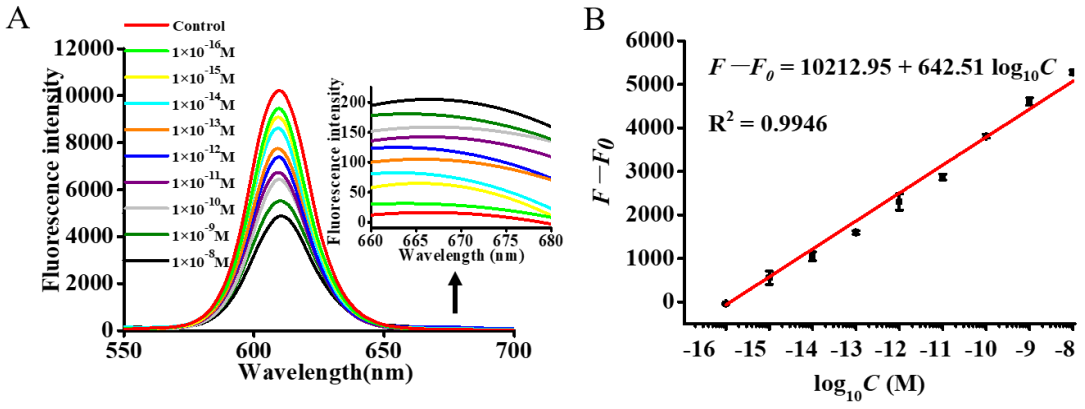

Figure S6. (A) Fluorescence emission spectra induced by different concentration miRNA-155 in the range from 0 (control) to 10^{-8} M. The inset shows the magnified fluorescence spectra from 660 to 680nm. (B) Linear relationship between the $F_0 - F$ of QD and the logarithm of miRNA-155 concentrations at the excitation wavelength of 488 nm. The concentration of each DNA probes is 100 nM. Error bars are standard derivation obtained from three independent experiments.

Quantification of target miRNA-155 by standard quantitative reverse-transcriptase polymerase chain reaction (qRT-PCR).

We used the standard quantitative reverse-transcriptase polymerase chain reaction (qRT-PCR) method to quantify target miRNA-155 (Figure S7). The products were subjected to quantitative PCR analysis after the reverse transcription reaction of target miRNA-155. The real-time fluorescence curves in response to different-concentration miRNA-155 were shown in Figure S7A, and the data were analyzed using the comparative C_T (threshold cycle) method. As shown in S7B, the C_T value exhibits a linear correlation with the logarithm of miRNA-155 concentration in the range from 1×10^{-13} to 1×10^{-9} M, and the regression equation is $C_T = -29.60 - 5.02 \log_{10} C_{\text{miRNA-155}}$ with a correlation coefficient (R^2) of 0.9981, where $C_{\text{miRNA-155}}$ is the concentration of target miRNA-155.

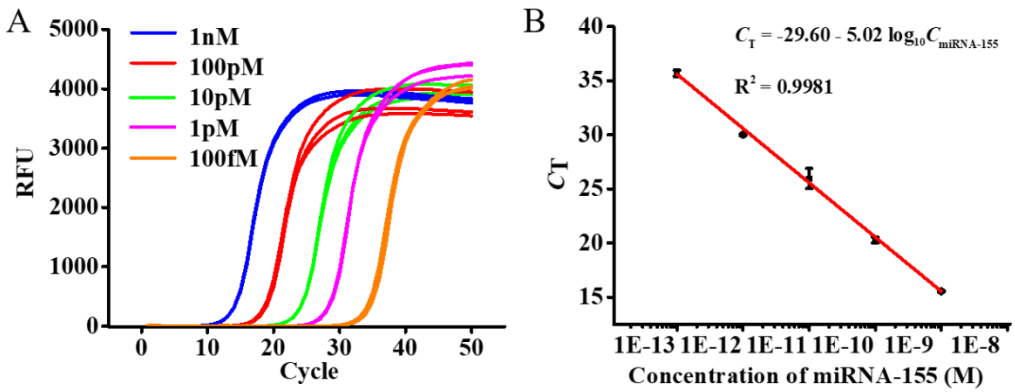

Figure S7. (A) Real-time fluorescence monitoring of the PCR amplification reaction in response to increasing concentrations of miRNA-155 from 1×10^{-13} to 1×10^{-9} M. RFU represents the relative fluorescence units. (B) Linear relationship of threshold cycle (C_T) value obtained from the data (A) as a function of the logarithm of miRNA-155. Error bars show the standard deviation of three experiments.

Table S1. Recovery study of miRNA-155 in 10% fetal bovine serum samples.

added (pM)	determined (pM)	recovery ratio (*R*1) (%)	RSD (%)
1000	992.1	99.20	1.88
100	100.78	100.78	3.28
10	9.91	99.10	5.05

References

（1）Ko, S. H.; Gallatin, G. M.; Liddle, J. A. Nanomanufacturing with DNA Origami: Factors Affecting the Kinetics and Yield of Quantum Dot Binding. *Adv. Funct. Mater.* **2012,** *22*, 1015-1023.

（2）Hildebrandt, N. Biofunctional Quantum Dots: Controlled Conjugation for Multiplexed Biosensors. *ACS Nano* **2011,** *5*, 5286-5290.